INTERNATIONAL JOURNAL OF LATEST TECHNOLOGY IN ENGINEERING, MANAGEMENT & APPLIED SCIENCE (IJLTEMAS)
ISSN 2278-2540 | DOI: 10.51583/IJLTEMAS | Volume XV, Issue VII, July 2026

Failure Analysis of Crankshaft with Variations of Defect Locations Using the Finite Element Method

Husaini[1]*, Ariel Alfansa[2], Teuku Arriessa Sukhairi[3] , Haris Darmawan[4]

Computational Mechanics Laboratory, Department of Mechanical Engineering, Universitas Syiah Kuala, Darussalam – Banda Aceh 23111, Indonesia

[*]Corresponding Author

DOI: https://doi.org/10.51583/IJLTEMAS.2026.150700082

Received: 29 July 2026; Accepted: 03 August 2026; Published: 13 August 2026

ABSTRACT

Crankshaft is a critical component in an internal combustion engine, operating under cyclic bending and torsional loads, making it susceptible to fatigue failure, particularly in regions with high stress concentration and pre-existing defects. Therefore, this study aimed to investigate the effect of defect location on the failure mechanism of the crankshaft using the Finite Element Method (FEM). The analysis was performed using ANSYS Student version of Mechanical on both defect-free and defective models. Defects were introduced at the crankpin fillet, main journal fillet, and oil hole. The material was specified as ASTM A536 Grade 80-55-06. The evaluated parameters included von Mises stress, strain, and Mode I stress intensity factor (K_I). The simulation results showed that the maximum von Mises stress in the defect-free model was 364.18 MPa, which is below the material yield strength of 379.2 MPa. In contrast, defective models produced K_I values ranging from 45 to 57 MPa√m, all exceeding the material fracture toughness (K_{IC}) of 32.9 MPa√m. The highest K_I value, 57 MPa√m, occurred at the main journal fillet with a crack depth of 0.6 mm. The results indicate that increasing crack depth elevates the likelihood of crack propagation and subsequent fatigue failure. Defect location exerts a significant influence on crankshaft failure behavior, and FEM provides an effective approach for predicting crack propagation in engine components.

Keywords : Crankshaft, stress analysis, finite element method, failure analysis, stress intensity factor.

INTRODUCTION

A crankshaft is a key component of an internal combustion engine, responsible for converting the reciprocating motion of the piston into rotary motion. During operation, it is subjected to repeated cyclic loading, making fatigue resistance a critical design consideration [1]. In pickup trucks, the crankshaft also plays an essential role in transmitting engine power through the drivetrain [2]. Operationally, the crankshaft operates under high rotational speeds and is subjected to combined bending and torsional stresses from combustion and inertial forces. Stress concentrations at the main journal, crankpin, fillet, and oil hole make these regions highly susceptible to fatigue failure [3].

The crankshaft, as the engine power shaft, works under a combination of cyclic bending and torsional loads, which produce tensile, compressive, and shear stresses on the crankpin radius and connecting rod seat [4]. Therefore, fatigue life prediction and stress concentration analysis are very important to ensure component reliability and safety [5]. Crankshaft materials are generally made of forged steel or cast iron according to strength requirements [6]. Cracks typically initiate at surface defects or regions of stress concentration and propagate under cyclic loading. Fillet regions are considered the most critical locations for fatigue failure [7].

Cracks initiate at stress concentration sites and propagate under cyclic loading, with fillets being the most critical regions for fatigue failure [7]. Previous studies indicate that crankshaft failure is primarily governed by fatigue mechanisms. Zulfikar (2018) reported that cracks initiated in the vicinity of the oil hole and propagated

ISSN 2278-2540 | DOI: 10.51583/IJLTEMAS | Volume XV, Issue VII, July 2026

under cyclic loading. However, the influence of crack location on fatigue behavior was not examined [9]. Therefore, this study examines the influence of crack depth and location on fatigue characteristics.

METHODOLOGY

A crankshaft converts the reciprocating motion of the piston into rotary motion and transmits engine power to the drivetrain. Typically manufactured from steel or cast iron, it is designed to withstand high mechanical loads. Figure 1 presents a failed crankshaft from a diesel pickup truck.

The components on the crankshaft consist of the crank pin, crank journal, crank arm, crankshaft bearing, balance weight, and oil hole.

Fig. 1. Crankshaft

Fig. 2. Crankshaft and its components [10]

This study used a crankshaft made of ASTM A536 Grade 80-55-06, which was selected because it is suitable for components operating under cyclic loads. The mechanical properties of this material directly affect the results of stress and strain analysis, as shown in Table 1.

TABLE I Properties of ASTM A536 Grade 80-55-06 Material [11]

Mechanical properties	Mark	Unit
Tensile strength (σ_u)	551	MPa
Poisson ratio(v)	0.30	-
Density (ρ)	7300	Kg/cm3
Modulus of elasticity (E)	172.4	GPa
Yield strength (σ_{ys})	379.2	MPa
Hardness, Rockwell B	89.5	HRB
Fracture Toughness (K_{IC})	33	MPa√m

ISSN 2278-2540 | DOI: 10.51583/IJLTEMAS | Volume XV, Issue VII, July 2026

The fracture toughness (K_{IC}) value of ASTM A536 Grade 80-55-06 material is 32.89 MPa√m, which has been studied previously [12].

Crankshaft modeling was performed using Autodesk Inventor based on predetermined dimensions. The model was created in two conditions, namely without defects and with defects, as independent variables of the study, as shown in Figure 3.

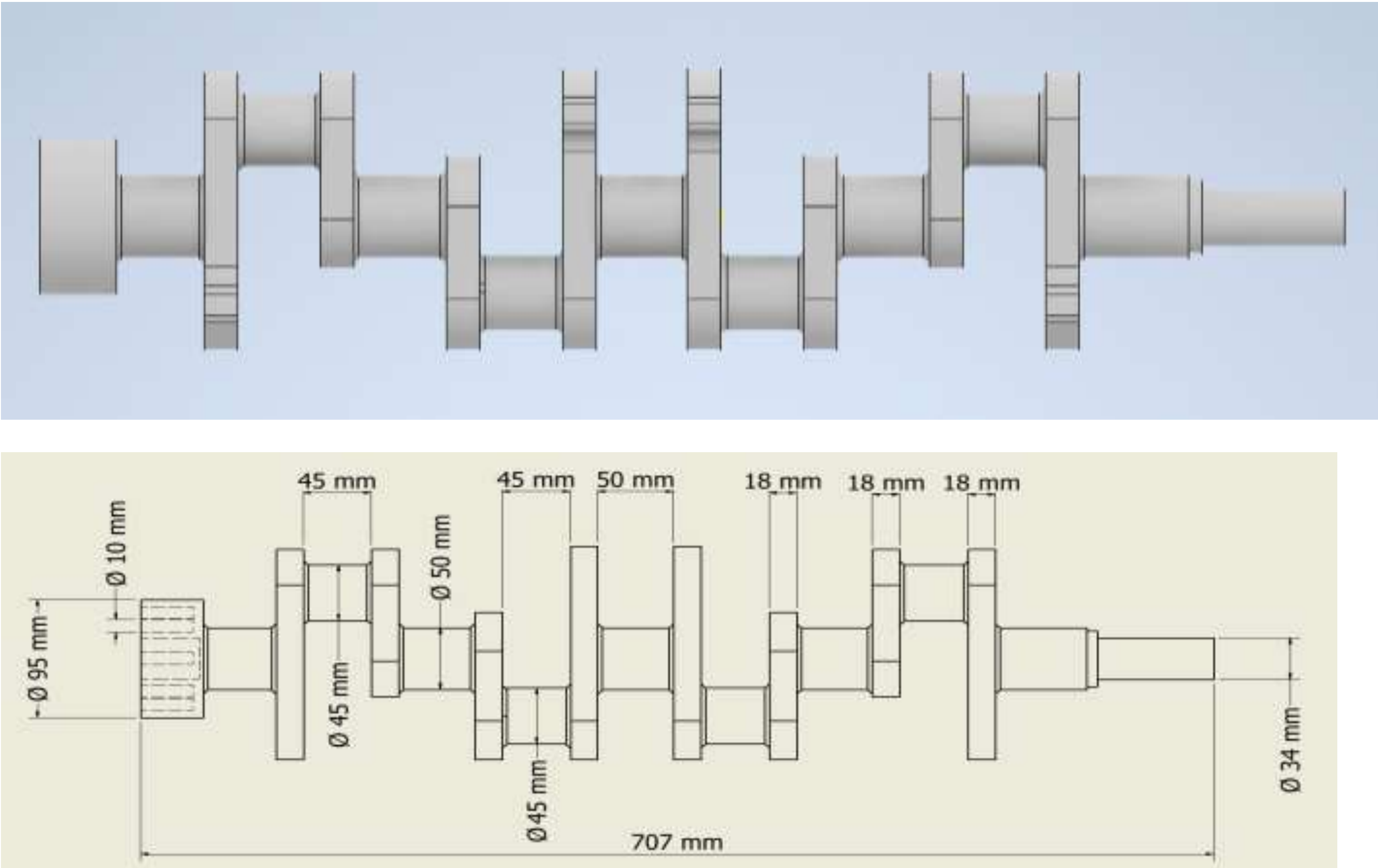

Fig. 3. 3D Dimensions of the Crankshaft

The initial defect dimensions of the crankshaft can be seen in Figure 4.

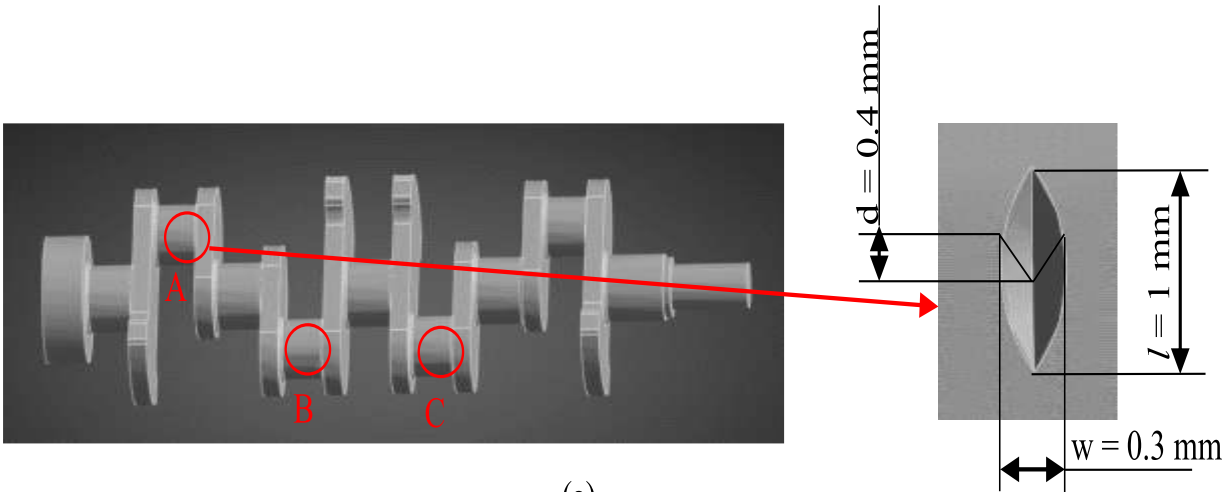

(a)

ISSN 2278-2540 | DOI: 10.51583/IJLTEMAS | Volume XV, Issue VII, July 2026

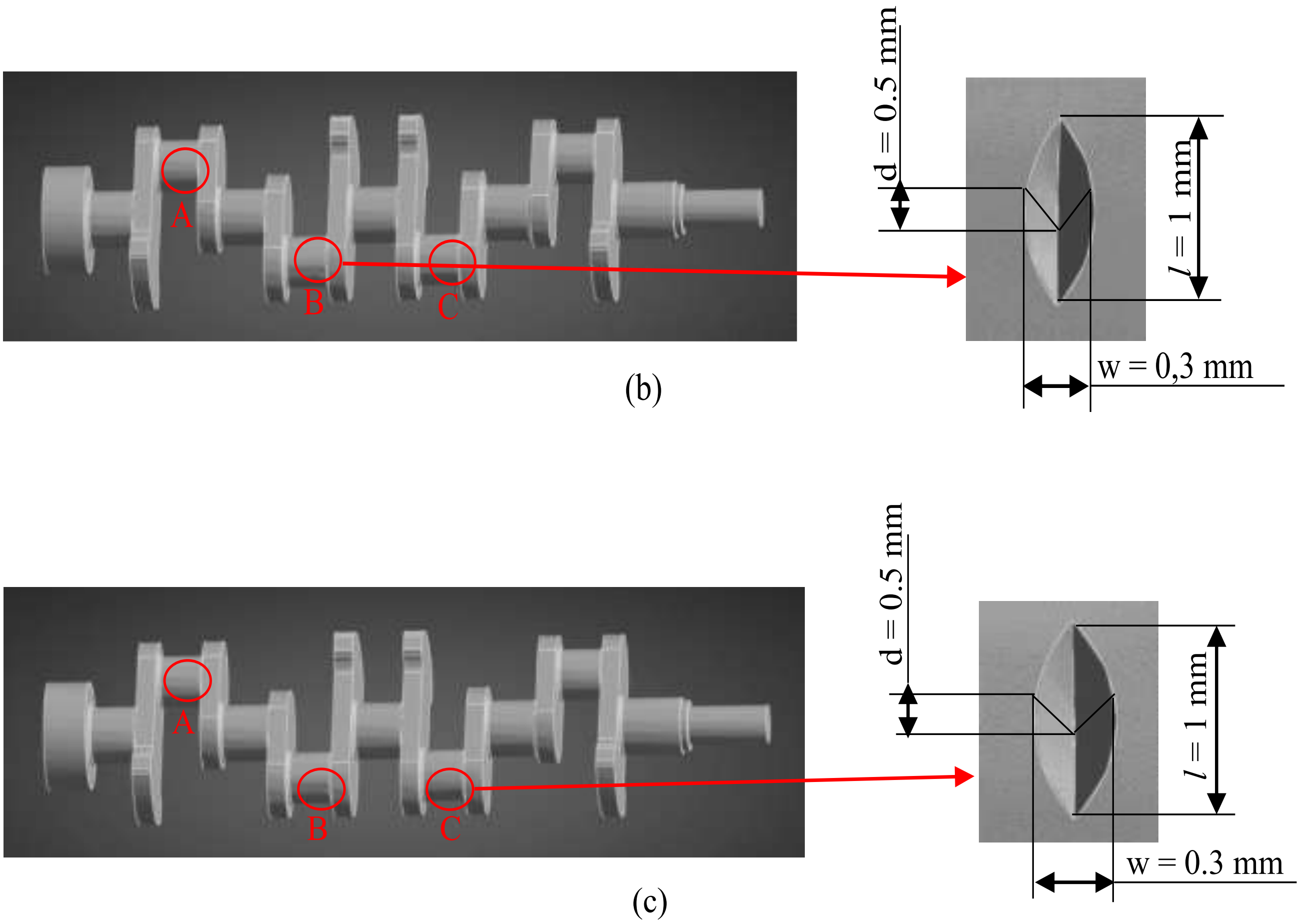

Fig. 4. Variations in defect locations, a) Initial defect condition at the crankpin fillet, b) Initial defect condition at the main journal fillet, c) Initial defect condition at the oil hole.

FEM is used to analyze stress and deformation statically and dynamically [13]. In this study, the analysis was performed using ANSYS Student version 2025. A crankshaft model from Autodesk Inventor was imported in STEP format, given ASTM A536 Grade 80-55-06 material properties, and then meshing was performed before numerical analysis.

Boundary condition applied with fixed support at both ends of the crankshaft and a pressure load of 300 MPa on the three surfaces of the crank pin [14-17]. The same loading was used for all models to evaluate the effects of crack location and depth on stress, strain, and stress intensity factor (K_I), as shown in Figure 5.

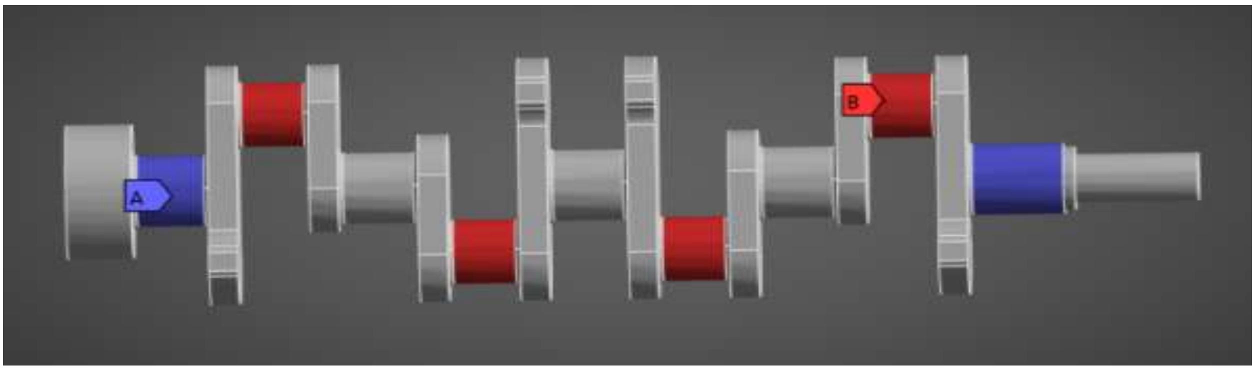

Fig. 5. Application of boundary conditions: (a) Fixed Support (A) on the Main Journal and (b) Loading Force on the Crank Pin (B)

ISSN 2278-2540 | DOI: 10.51583/IJLTEMAS | Volume XV, Issue VII, July 2026

Stress Intensity Factor (K_I) is a linear crack mechanics parameter that describes stress concentration at the crack tip [18-21]. In this study, the K_I value was obtained using ANSYS through the J-integral method and displacement around the crack tip, then compared with the material fracture toughness (K_{IC}). If $K_I \geq K_{IC}$, then the crack is predicted to experience propagation.

RESULTS AND DISCUSSION

Analysis using FEM was carried out to evaluate the distribution of stress and strain that occurs in the component.

The simulation results of the flawless model show a maximum stress of 364.18 MPa in the critical area of the crankshaft, and a minimum stress of 3.635e-8 MPa in the location that does not receive significant loading, as shown in Figure 6. The maximum stress value remains below the yield strength of ASTM A536 Grade 80-55-06 (379.2 MPa). Therefore, the crankshaft operates in the elastic region and can be considered structurally safe under the given loading conditions. A flawless model is used as a reference to analyze the effect of cracks on the distribution of stress, strain, and stress intensity factor (K_I).

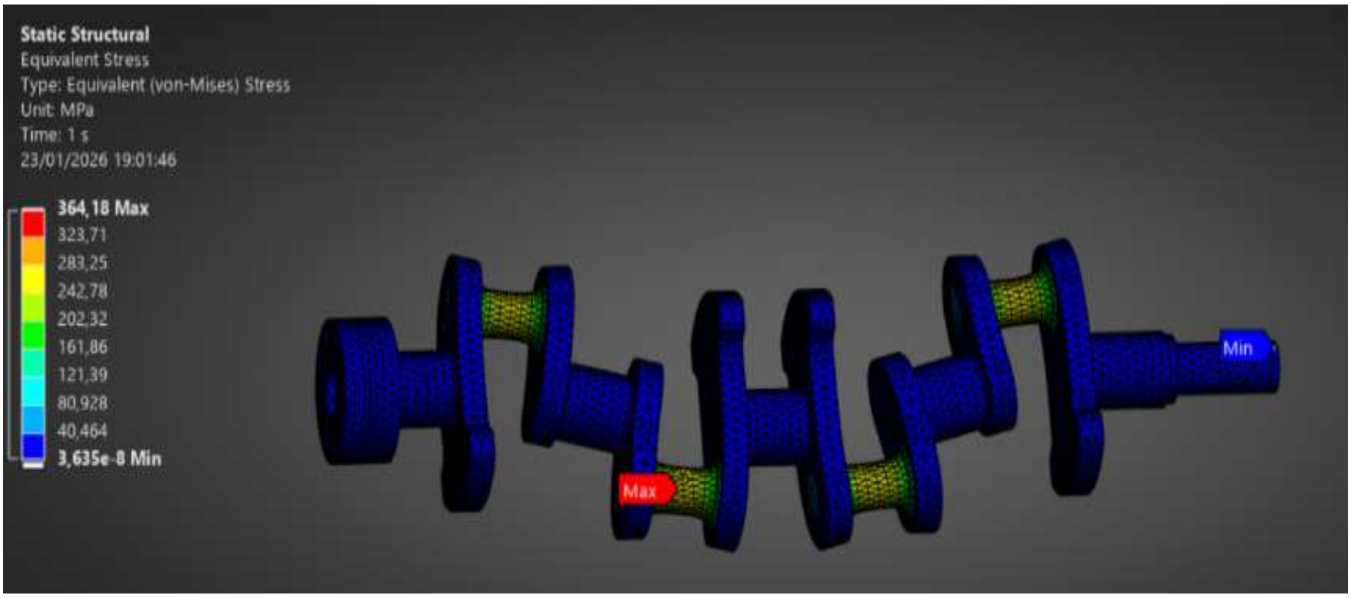

Fig. 6. Results of von Mises stress without defects

Based on the analysis results, it shows that increasing the depth of the defect from 0.4 mm, 0.5 mm, and 0.6 mm at location A increases the stress value and stress intensity factor (K_I), which can be seen in Table 2. Increasing crack depth leads to higher stress concentration at the crack tip, thereby enhancing the likelihood of crack propagation.

TABLE II The effect of defect depth on stress value and Mode I stress intensity factor at defect location A.

Defect Location	Defect Length (mm)	Defect Width (mm)	Defect Depth (mm)	Stress Value (MPa)	K_{IC} Value (MPa√m)
A	1	0.3	0.4	85618	32.89
A	1	0.3	0.5	94181	32.89
A	1	0.3	0.6	102740	32.89

ISSN 2278-2540 | DOI: 10.51583/IJLTEMAS | Volume XV, Issue VII, July 2026

The simulation results show that increasing crack depth increases stress around the crack tip. Stress increased from 85618 at a crack depth of 0.4 mm to 94181 at 0.5 mm and reached 1.02740 at 0.6 mm due to higher stress concentration. Figure 7 shows that the 0.6 mm crack depth produced the highest stress.

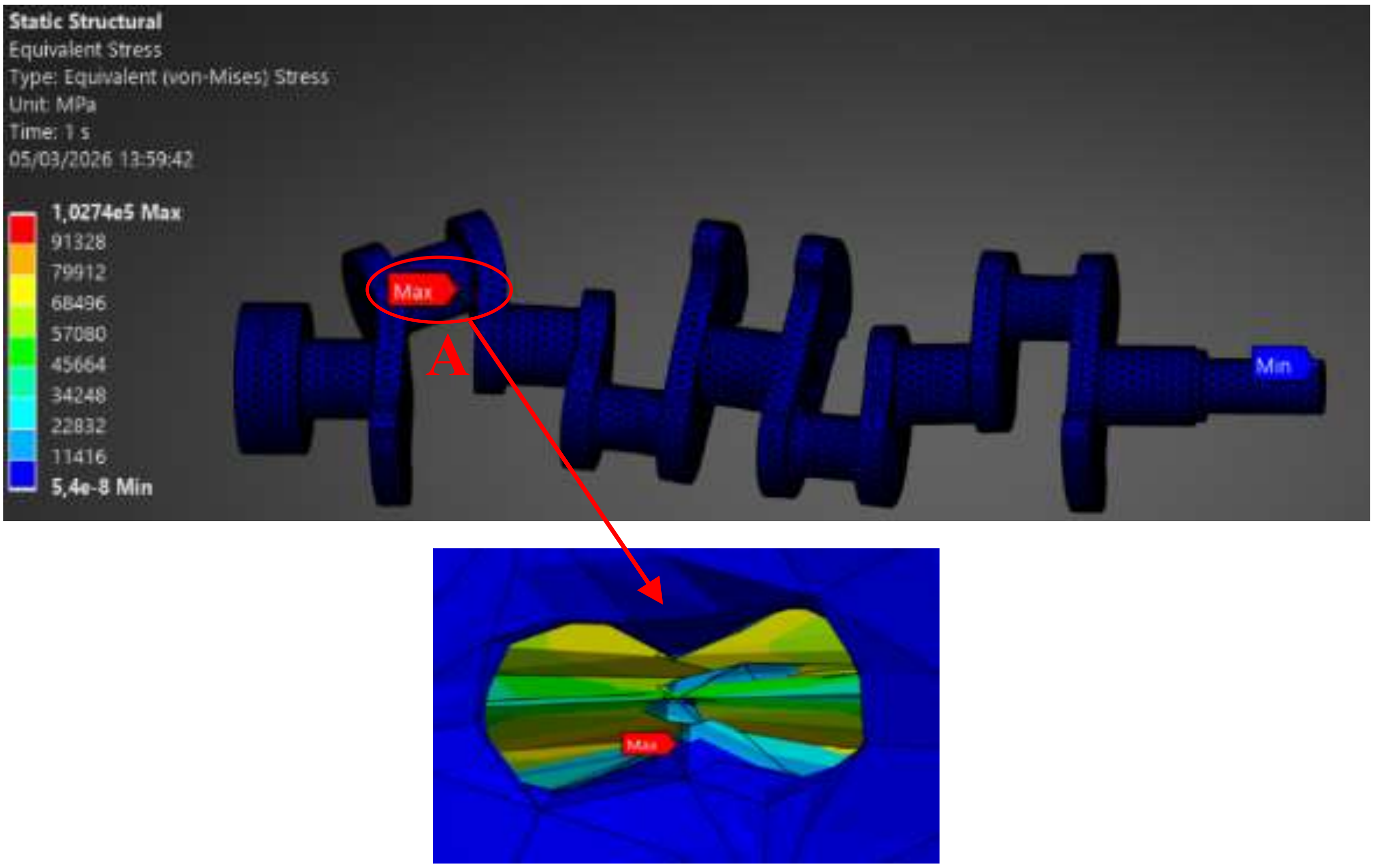

Fig. 7. Distribution of von Mises stress at defect location A with a crack depth of 0.6 mm as the most critical condition with the highest stress value

The results of stress intensity factor (K_I) analysis at location A (crank pin fillet) with varying defect depths are presented in Table 3. K_I value is used to determine the effect of increasing defect depth on the tendency of cracks to propagate. The greater the K_I value, the higher the possibility of cracks developing on the crankshaft.

TABLE III Results of Stress Intensity Factor (K_I) Analysis of Defect Depth Variations at Location A

Defect Location	Defect Depth (mm)	Node	K_I Value (MPa$\sqrt{mm}$)	K_I Value (MPa$\sqrt{m}$)	K_{IC} Value (MPa$\sqrt{m}$)
A	0.4	105786	1427.8	45	32.89
A	0.5	105748	1570.7	50	32.89
A	0.6	105796	1713.5	54	32.89

Stress intensity factor (K_I) value also increases with increasing crack depth. At a depth of 0.4 mm, the K_I value is 45 MPa$\sqrt{m}$, increasing to 50 MPa$\sqrt{m}$ at a depth of 0.5 mm, and reaching 54 MPa$\sqrt{m}$ at a depth of 0.6 mm, as seen in Figure 8. An increase in stress intensity factor (K_I) indicates a higher stress concentration at the crack tip, thereby increasing the propensity for crack propagation.

ISSN 2278-2540 | DOI: 10.51583/IJLTEMAS | Volume XV, Issue VII, July 2026

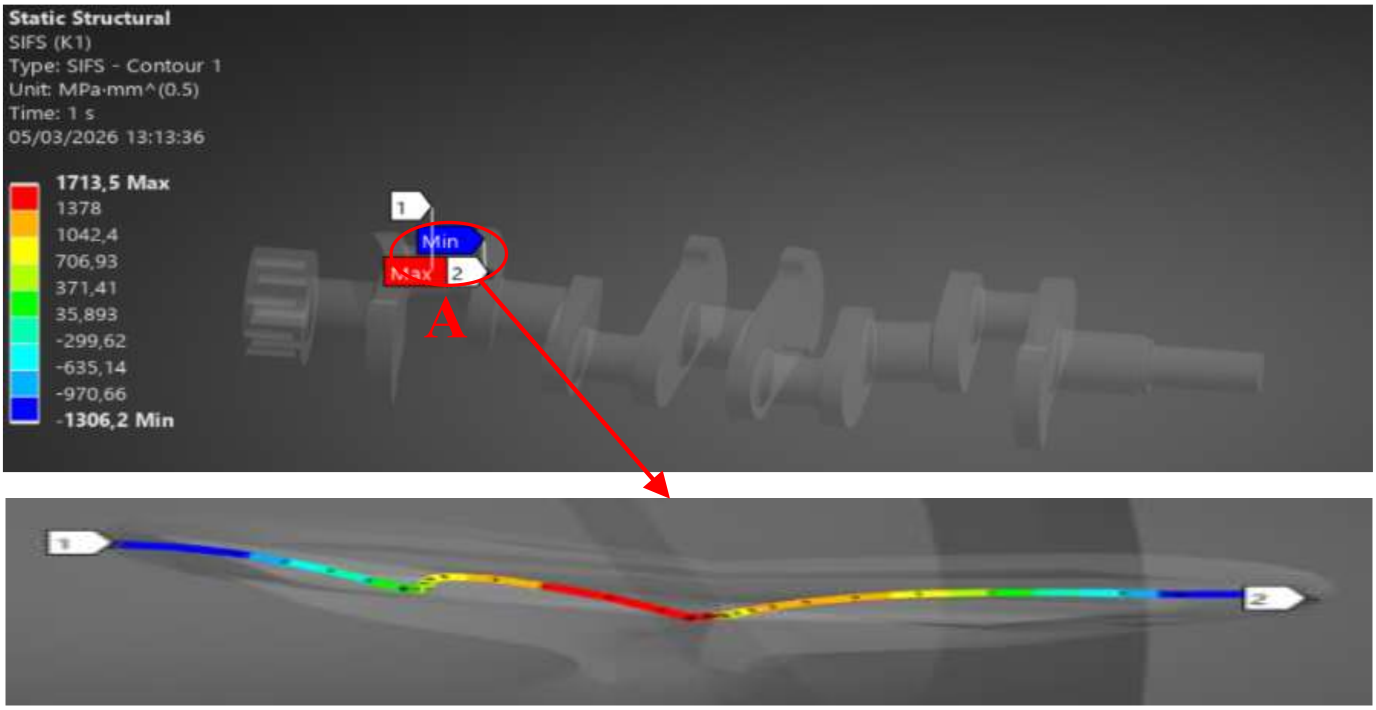

Fig. 8. Simulation results of stress intensity factor (K_I) on crack propagation at defect location A with a crack depth of 0.6 mm as the most critical condition

Analysis at location B was performed by varying defect depth to evaluate changes in stress values and stress intensity factors (K_I). The results obtained are presented in Table 4.

TABLE IV Effect of defect (crack) depth on stress value and Mode I stress intensity factor (K_I) at defect location B.

Defect Location	Defect Length (mm)	Defect Width (mm)	Defect Depth (mm)	Stress Value (MPa)	K_{IC} Value (MPa√m)
A	1	0.3	0.4	102740	32.89
A	1	0.3	0.5	111310	32.89
A	1	0.3	0.6	119870	32.89

The simulation results show that stress at location B increased with crack depth, rising from 1.02740 at 0.4 mm to 1.11310 at 0.5 mm and 1.19870 at 0.6 mm. Figure 9 shows that the 0.6 mm crack depth produced the highest stress due to increased stress concentration at the crack tip.

ISSN 2278-2540 | DOI: 10.51583/IJLTEMAS | Volume XV, Issue VII, July 2026

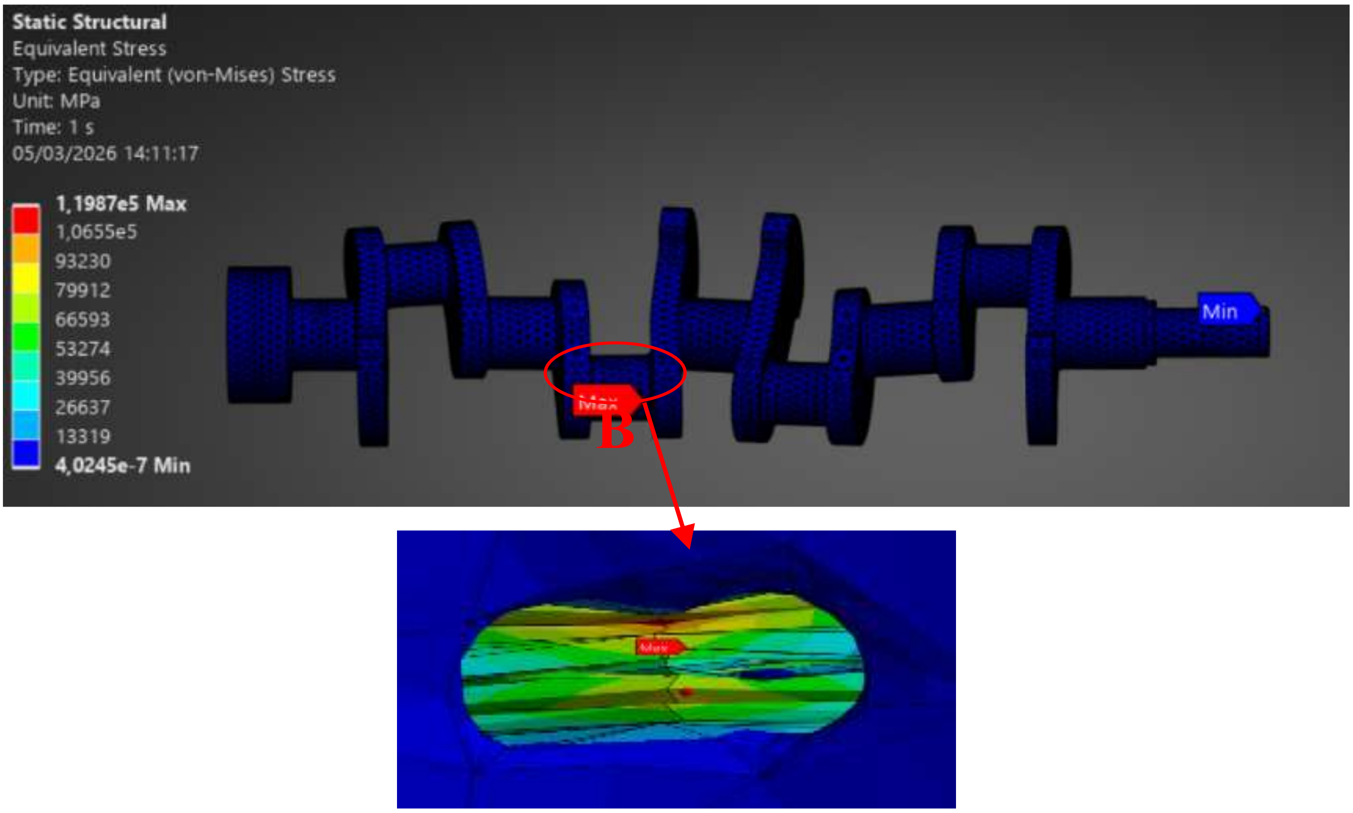

Fig. 9. Distribution of von Mises stress at defect location B with a crack depth of 0.6 mm as the most critical condition with the highest stress value

Based on stress distribution results at location B, the analysis continued by calculating the stress intensity factor (K_I) at each variation of defect depth. The obtained K_I values are presented in Table 5 as the tendency of crack propagation on the crankshaft.

TABLE V Results of Stress Intensity Factor (K_I) Analysis of Defect Depth Variations at Location B.

Defect Location	Defect Depth (mm)	Node	K_I Value (MPa√mm)	K_I Value (MPa√m)	K_{IC} Value (MPa√m)
B	0.4	105726	1545.5	49	32.89
B	0.5	105764	1674.3	53	32.89
B	0.6	105924	1803.1	57	32.89

Stress intensity factor (K_I) at location B increased with crack depth, from 49 MPa√m at 0.4 mm to 53 MPa√m at 0.5 mm and 57 MPa√m at 0.6 mm. Figure 10 shows that increasing crack depth raises K_I, indicating a greater tendency for crack propagation.

ISSN 2278-2540 | DOI: 10.51583/IJLTEMAS | Volume XV, Issue VII, July 2026

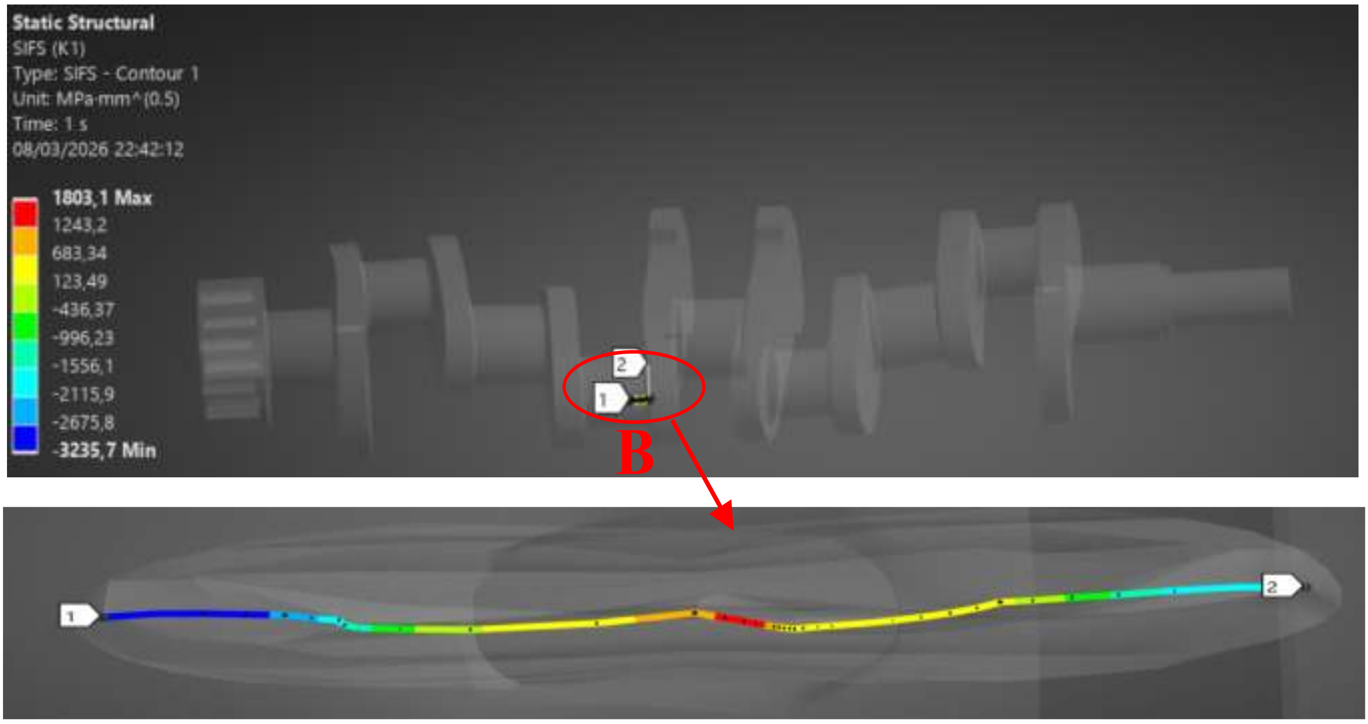

Fig. 10. Simulation results of stress intensity factor (K_I) on crack propagation at defect location B with a crack depth of 0.6 mm as the most critical condition

Analysis at defect location C was performed by varying crack depth to observe changes in stress values and stress intensity factors (K_I). The results of this analysis are presented in Table 6.

TABLE VI Effect of defect (crack) depth on stress value and Mode I stress intensity factor (K_I) at defect location C.

Defect Location	Defect Length (mm)	Defect Width (mm)	Defect Depth (mm)	Stress Value (MPa)	K_{IC} Value (MPa√m)
C	1	0.3	0.4	82502	32.89
C	1	0.3	0.5	89376	32.89
C	1	0.3	0.6	96251	32.89

The simulation results show that stress at location C increased with crack depth, from 82502 at 0.4 mm to 89376 at 0.5 mm and 96251 at 0.6 mm. Figure 11 shows that the 0.6 mm crack depth produced the highest stress due to increased stress concentration at the crack tip.

ISSN 2278-2540 | DOI: 10.51583/IJLTEMAS | Volume XV, Issue VII, July 2026

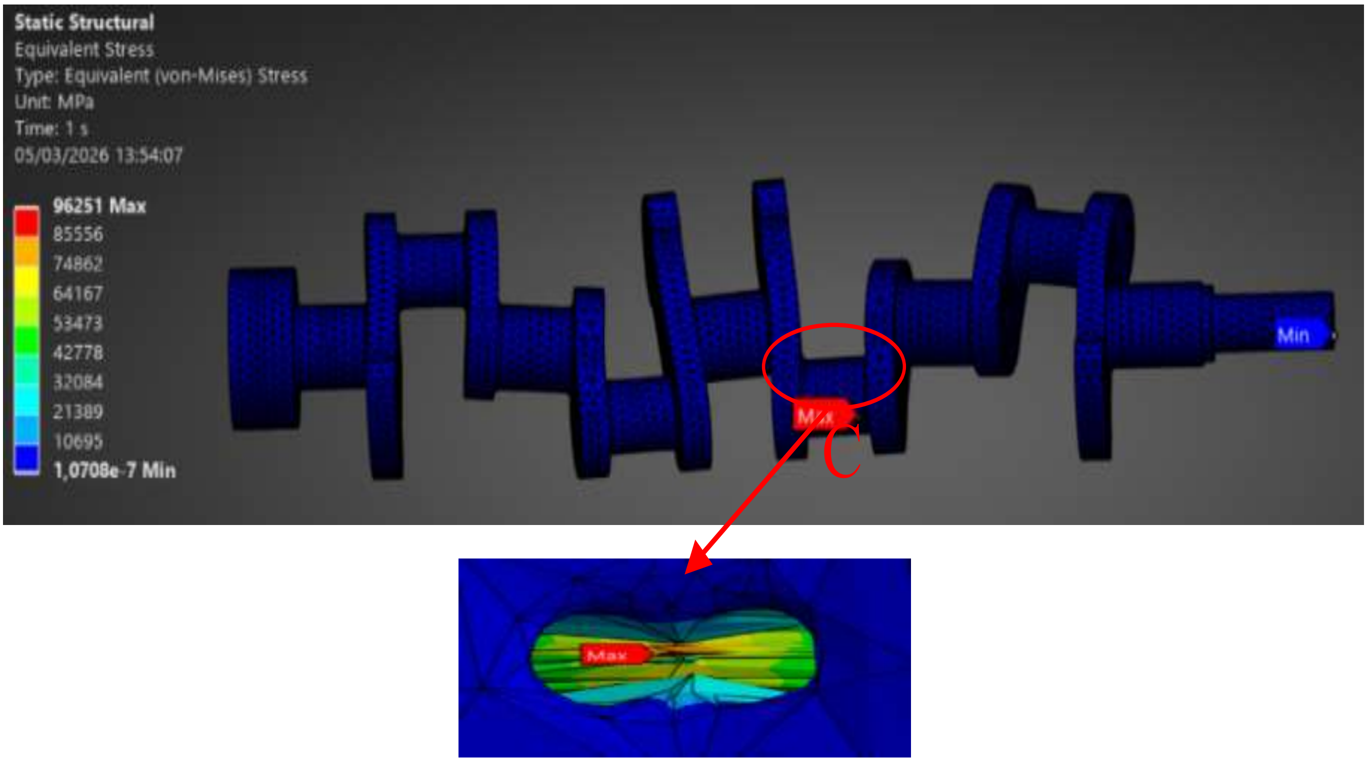

Fig. 11. Distribution of von Mises stress at defect location C with a crack depth of 0.6 mm as the most critical condition with the highest stress value

Based on the results of stress distribution analysis at location C, stress intensity factor (K_I) was calculated for each variation in defect depth. The results of these calculations are presented in Table 7.

TABLE VII Results of Stress Intensity Factor (K_I) Analysis of Defect Depth Variations at Location C.

Defect Location	Defect Depth (mm)	Node	K_I Value (MPa√mm)	K_I Value (MPa√m)	K_{IC} Value (MPa√m)
C	0.4	105786	1537.5	48	32.89
C	0.5	105775	1665.6	53	32.89
C	0.6	105886	1793.6	56	32.89

The simulation results show that the stress intensity factor (K_I) value also increases with increasing crack depth, as shown in Figure 12. At a crack depth of 0.4 mm, the K_I value is 48 MPa√m, then increases to 53 MPa√m at a depth of 0.5 mm, and reaches 56 MPa√m at a depth of 0.6 mm.

ISSN 2278-2540 | DOI: 10.51583/IJLTEMAS | Volume XV, Issue VII, July 2026

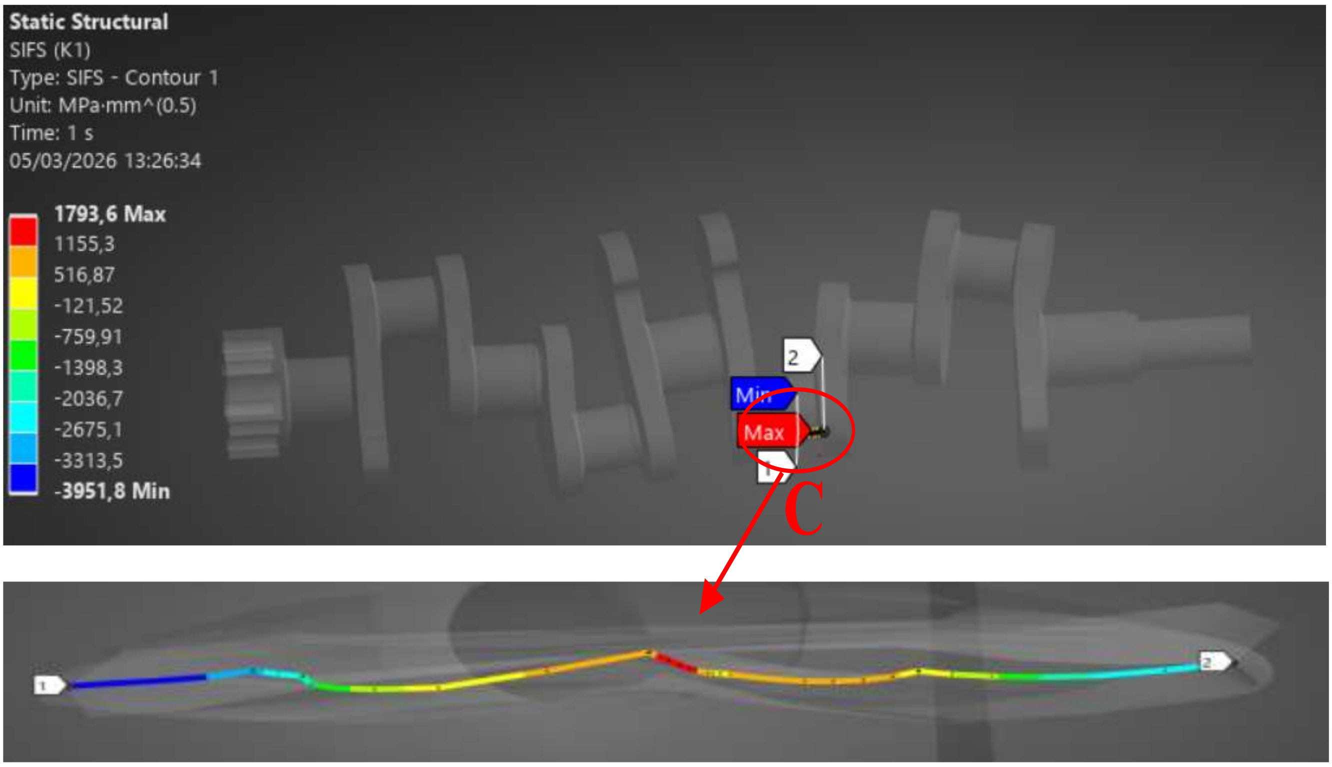

Fig. 12. Simulation results of the stress intensity factor (K_I) on crack propagation at defect location C with a crack depth of 0.6 mm as the most critical condition

This analysis compares the effect of variations in defect location on the Mode I stress intensity factor (K_I) value on a crankshaft with the same crack depth. The locations analyzed include A (crank pin fillet), B (main journal fillet), and C (oil hole). Differences in geometry and stress distribution at each location result in different K_I values, where the higher the K_I value, the greater the potential for crack propagation in the material.

Comparison of stress intensity factor (K_I) values against material fracture toughness (K_{IC}) at various defect locations with a depth of 0.4 can be seen in Table 8.

TABLE VIII Comparison of Stress and Strain K_I Values Against Variations in Defect Locations with a Depth of 0.4

Defect Location	Defect Length (mm)	Defect Width (mm)	Defect Depth (mm)	Stress Value (MPa)	K_I Value (MPa√m)	K_{IC} Value (MPa√m)
A	1	0.3	0.4	85618	45	32.89
B	1	0.3	0.4	102740	49	32.89
C	1	0.3	0.4	82502	48	32.89

Table 8 shows that stress intensity factor (K_I) varies with defect location. Location B has the highest K_I (49 MPa√m), followed by location C (48 MPa√m) and location A (45 MPa√m), indicating the greatest crack propagation potential at a crack depth of 0.4 mm. K_I comparison is shown in Figure 13.

ISSN 2278-2540 | DOI: 10.51583/IJLTEMAS | Volume XV, Issue VII, July 2026

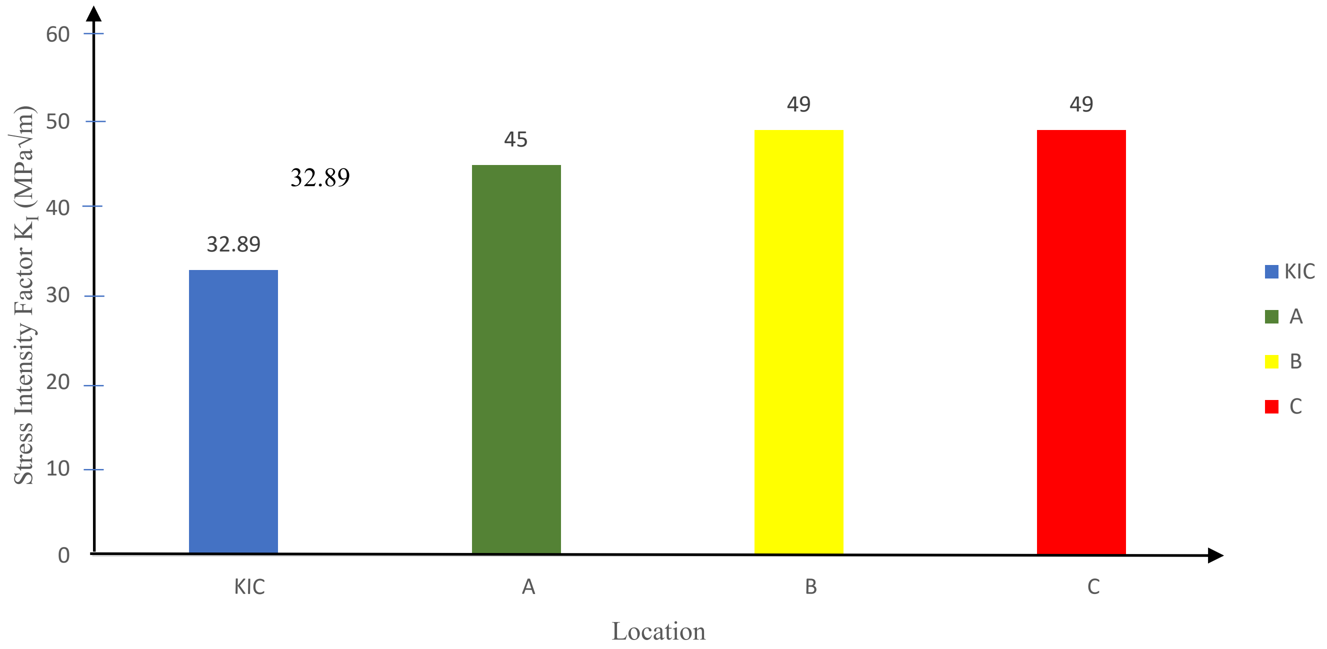

Fig. 13. Comparison graph of K_I with K_{IC} for each defect model at a d epth of 0.4 mm

Based on Figure 13, all stress intensity factor (K_I) values exceed the material fracture toughness (K_{IC}) value of 32.89 MPa√m. K_I values at locations A, B, and C are 45 MPa√m, 49 MPa√m, and 48 MPa√m, Location B has the highest K_I, and all locations exceed K_{IC}, indicating crack propagation potential.

Comparison of stress intensity factor (K_I) and material fracture toughness (K_{IC}) values at various defect locations with a crack depth of 0.5 mm is presented in Table 9.

TABLE IX Comparison of Stress and Strain K_I Values Against Variations in Defect Locations with a Depth of 0.5

Defect Location	Defect Length (mm)	Defect Width (mm)	Defect Depth (mm)	Stress Value (MPa)	K_I Value (MPa√m)	K_{IC} Value (MPa√m)
A	1	0.3	0.5	94181	50	32.89
B	1	0.3	0.5	111310	53	32.89
C	1	0.3	0.5	89376	53	32.89

Based on Table 9, stress intensity factor (K_I) increased at all locations with crack depth. Locations B and C exhibited the highest K_I (53 MPa√m), while location A reached 50 MPa√m, indicating greater crack propagation potential, and K_I comparison is presented in Figure 14.

ISSN 2278-2540 | DOI: 10.51583/IJLTEMAS | Volume XV, Issue VII, July 2026

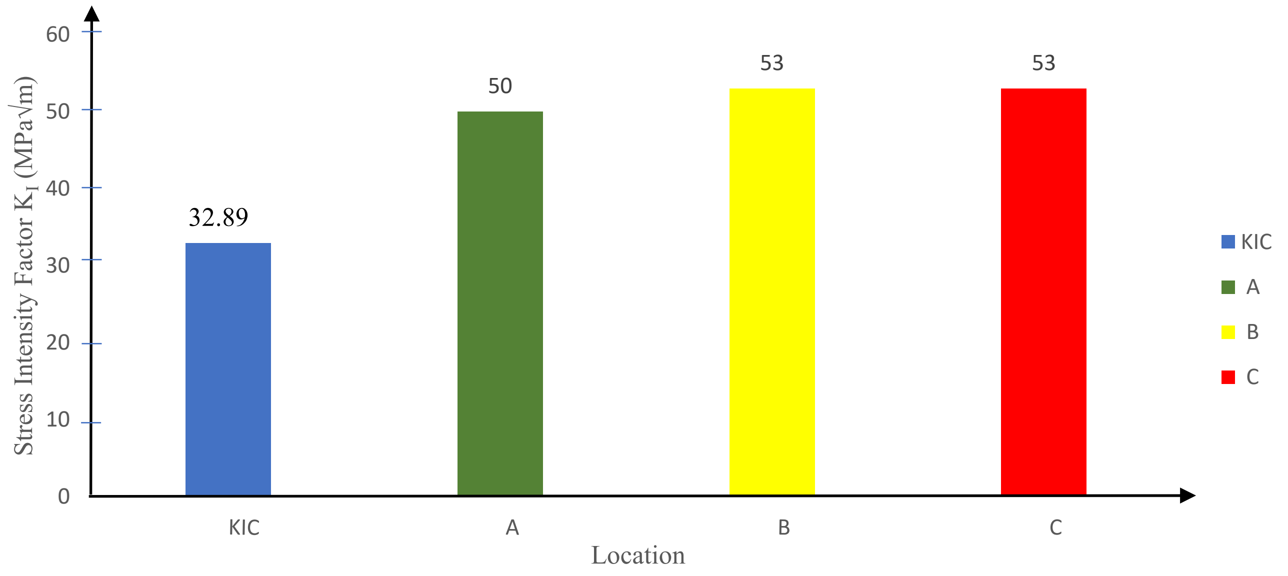

Fig. 14. Comparison graph of K_I with K_{IC} for each defect model at a depth of 0.5 mm

Based on Figure 14, all stress intensity factor (K_I) values exceed the material fracture toughness (K_{IC}) of 32.89 MPa√m. Locations B and C have the highest K_I (53 MPa√m), while location A reaches 50 MPa√m, indicating crack propagation potential at all locations.

The effect of defect location on stress intensity factor (K_I) value at crack depth of 0.6 mm can be observed through a comparison with the material fracture toughness (K_{IC}) value presented in Table 10.

TABLE X Comparison Values of Stress and Strain K_I Against Variations in Defect Locations with a Depth of 0.6

Defect Location	Defect Length (mm)	Defect Width (mm)	Defect Depth (mm)	Stress Value (MPa)	K_I Value (MPa√m)	K_{IC} Value (MPa√m)
A	1	0.3	0.6	102740	54	32.89
B	1	0.3	0.6	119870	57	32.89
C	1	0.3	0.6	96251	56	32.89

Based on Table 10, stress intensity factor (K_I) increased at all locations with crack depth. Location B exhibited the highest K_I (57 MPa√m), followed by location C (56 MPa√m) and location A (54 MPa√m), making it the most critical location for crack propagation, and K_I comparison is shown in Figure 15.

ISSN 2278-2540 | DOI: 10.51583/IJLTEMAS | Volume XV, Issue VII, July 2026

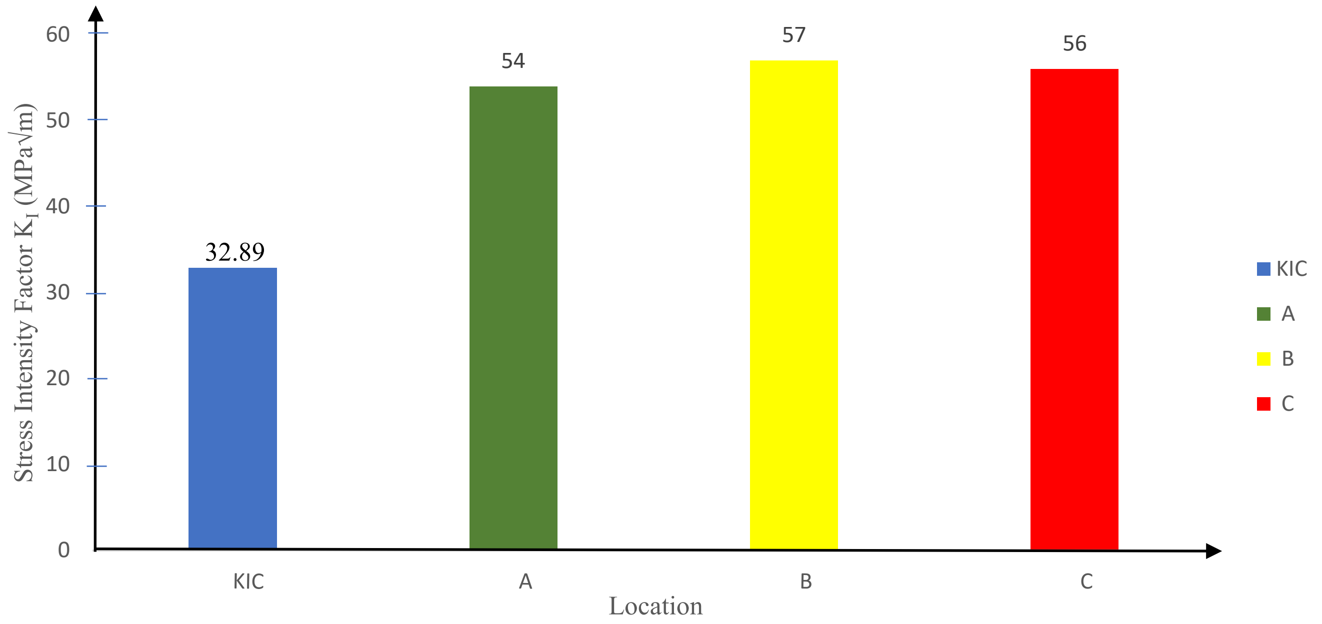

Fig. 15. Comparison Graph of K_I with K_{IC} for each defect model at a depth of 0.6 mm

Based on Figure 15, all stress intensity factor (K_I) values exceed the material fracture toughness (K_{IC}) of 32.89 MPa√m. Location B has the highest K_I (57 MPa√m), followed by location C (56 MPa√m) and location A (54 MPa√m), making it the most critical location for crack propagation.

Simulation results show that defect location affects stress intensity factor (K_I). Location B has the highest K_I and is the most critical area, while location A has the lowest. K_I increased at all locations with crack depth. K_I comparison is shown in Figure 16.

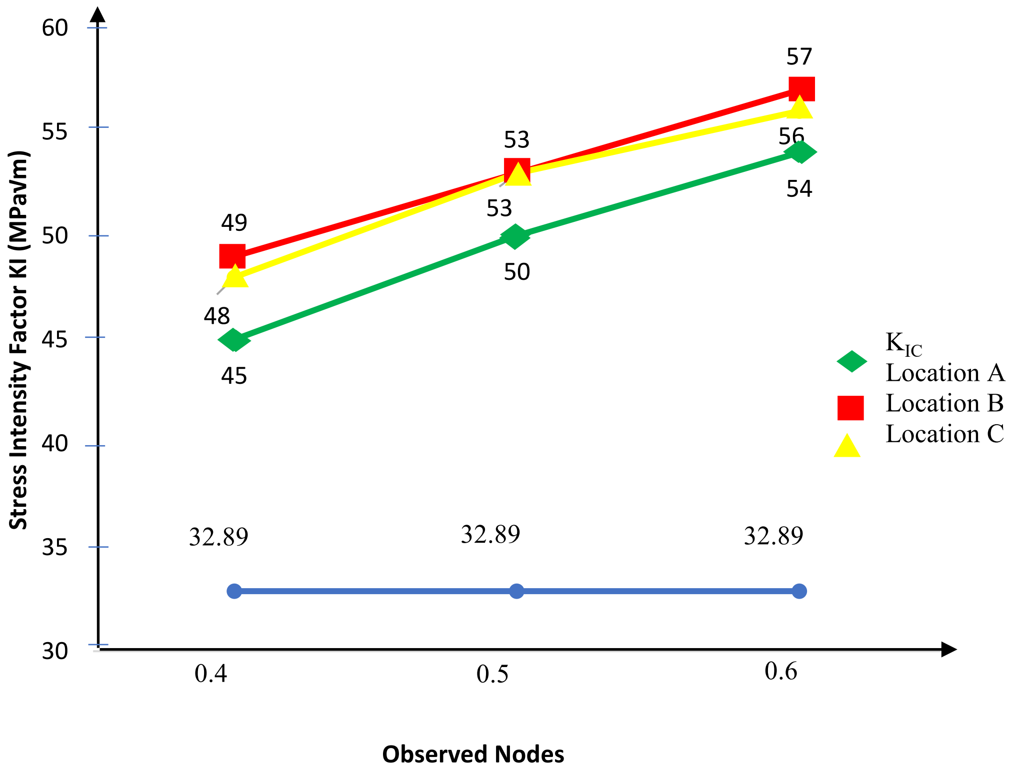

Fig. 16. Comparison graph of K_I with K_{IC} at each depth of the defect model

The graph shows that stress intensity factor (K_I) values at all defect locations increase with increasing crack depth, and all exceed the material fracture toughness (K_{IC}) value of 32.89 MPa√m. Location B was the most critical area, exhibiting the highest K_I values.

This study's findings are consistent with those reported by Zhang [22], who stated that the presence of an initial defect in the fillet region crack propagation, ultimately leading to material failure. Similarly, a study conducted by Witek [23] also reported that the failure occurred due to the presence of an initial defect in the crankpin of the crankshaft.

CONCLUSSION

In conclusion, this study showed that all stress intensity factor (K_I) values obtained from the simulations (45–57 MPa√m) exceed the material fracture toughness (K_{IC}) of 32.89 MPa√m (ASTM A536 Grade 80-55-06), indicating a potential for crack propagation. Increasing crack depth elevates stress intensity factor (K_I) at all locations. The main journal fillet represents the most critical region, exhibiting the highest K_I value of 57 MPa√m at a crack depth of 0.6 mm. This is consistent with the findings of the present study, in which the defect was also modeled in the crank pin region, and the results demonstrated the occurrence of failure.

This study has several limitations. The finite element analysis was conducted under simplified static loading conditions and assumed homogeneous, isotropic material properties without considering cyclic loading.

ACKNOWLEDGEMENTS

This work was supported by a research grant from the Ministry of Research, Technology, and Education, Republic of Indonesia, and the Institute for Research and Community Services (LPPM) Universitas Syiah Kuala. The authors also wish to extend their gratitude to the Computational Mechanics Laboratory of the Department of Mechanical Engineering for providing the necessary facilities and support.

REFERENCES

1. Metkar, A., RM Sunnapwar, and SD Hiwase. (2011). Review: Fatigue analysis and estimated life of crankshafts. Int. J. Mech. Eng. Mater., Vol. 6, no. 3, pp. 425–430.
2. Prasetya, T., Sarifuddin, and BJ Raharjo. (2018). Crank Pin Journal Crankshaft Wear on Diesel Engine Generator on MV. Kartini Baruna. J. Bahari Dynamics, Vol. 9, pp. 2126–2136.
3. Çevik, G., and R. Gürbüz. (2013). Evaluation of fatigue performance of a fillet rolled diesel engine crankshaft. Eng. File. Anal., Vol. 27, pp. 250–261.
4. Chetan Kahate, Ashok Keche, (2016) "Failure analysis of crankshaft using finite element approach," International Journal of Engineering and Applied Sciences (IJEAS), Vol. 3, no. 4, pp. 46–49.
5. Paswan, MK, and AK Goel. (2008). Fatigue testing procedure of six-cylinder diesel engine crankshaft. ARISER, Vol. 3, pp. 144–151.
6. LL Myagkov, K. Mahkamov, ND Chainov, and I. Mankamova, (2014) "Advanced and Conventional Internal Combustion Engine Materials," in Alternative Fuels and Advanced Vehicle Technologies for Improved Environmental Performance: Towards Zero Carbon Transportation, Elsevier, Ch. 11, pp. 370–392.
7. Husaini, M. Notomi, K. Kishimoto, and T. Shibuya. (1997). Crack initiation behavior of ABS resin under mode I and mixed mode loading. Materials Science Research International, Vol. 3, no. 3, pp. 158–165.
8. RM Metkar, VK Sunnapwar, and SD Hiwase, (2011) "A fatigue analysis and life estimation of crankshaft – A review," International Journal of Mechanical and Materials Engineering (IJMME), vol. 6, no. 3, pp. 425–430.
9. Husaini, TE Putra, and Zulfikar. (2018). Analysis of Cracks on a Fractured Surface of the Vehicle Crankshaft Using the Finite Element Method. International Journal of Engineering & Technology, Vol. 7, no. 4.36, pp. 1564–1568.

ISSN 2278-2540 | DOI: 10.51583/IJLTEMAS | Volume XV, Issue VII, July 2026

10. Abdullah, S., JC Choi, JA Giaconim, and JR Yates. (2006). Bump extraction algorithm for variable amplitude fatigue loading. Int. J. Fatigue, Vol. 28, pp. 675–691.
11. Information on DuraBar ASTM A536 Grade 80-55-06. Available at:https://www.dura-bar.com/products/ductile-iron-80-55-06.cfm.
12. Kai-Pen Jen, Joseph T. Scardina, and D.G. Smith. (1985). Fracture behavior of as-cast pearlite nodular iron. Mater. Sci. Eng., Vol. 22, no. 2, pp. 227–236.
13. Cook, R.D. (1990). Concepts and Applications of Finite Element Analysis. 2nd ed. Bandung, Indonesia: PT Eresco, pp. 4–9.
14. Husaini. (2015). Basics of Fracture Mechanics. Banda Aceh: Syiah Kuala University Press.
15. Husaini, R. Riantoni, N. Ali, & T. E. Putra. (2019). Failure Analysis of the Leaf Spring of Truck Colt Diesel Using Finite Element Method. IOP Conference Series: Materials Science and Engineering. 547. 012017.
16. Husaini, N. Ali, R. Riantoni, T. E. Putra & H. Husin. (2021). Study of leaf spring fracture behavior used in the suspension systems in the diesel truck vehicles. IOP Conf. Ser.: Mater. Sci. Eng. 541 012046.
17. Husaini, N. Ali & A. Bakhtiar. (2016). Analysis on The Surface of Broken Screw Spring Front Car Suspension. Proseding Seminar Nasional Teknologi Rekayasa (SNTR) III. 111-117.
18. Farzin, M., and S. Akhavan. (2014). Stress analysis of a crankshaft under dynamic loading. International Journal of the Iron & Steel Society of Iran, Vol. 11, no. 1, pp. 16–22.
19. T. E. Putra, Husaini, M. Ikbal. (2021). Automotive suspension component behaviors driven on flat and rough road surfaces. Heliyon, 7(7).
20. Husaini, N. Ali, J. K. Hamza & S. E. Sofyan. (2019). Effects of welding on the change of microstructure and mechanical properties of low carbon steel. IOP Conf. Series: Materials Science and Engineering 523.
21. T. E. Putra & Husaini. (2018). Identifying strain signal characteristics of automotive suspension system subjected to road surface vibrations. AIP Conf. Proc. 1983, 030004.
22. Zhang, H. Y., Qu, S., Dong, C., Fu, C. M., Zang, Q. S. and Zhang, Z. F.. "Failure Analysis of a Diesel Engine Crankshaft" Practical Metallography, vol. 58, no. 5, 2021, pp. 282-298. https://doi.org/10.1515/pm-2021-0020.
23. Witek, L. & Sikora, Michał & Stachowicz, Feliks & Trzepieciński, Tomasz. (2017). Stress and failure analysis of the crankshaft of diesel engine. Engineering Failure Analysis. 82. 10.1016/j.engfailanal.2017.06.001.